

Chapter 2

Carbon-Based Nanomaterials for Nanozymes

Abstract Carbon-based nanomaterials, such as fullerene, graphene, carbon nanotubes, and their derivatives, have been extensively studied to mimic various natural enzymes owing to their fascinating catalytic activities. In this chapter, their enzyme mimetic activities (such as nuclease mimics, superoxide dismutase mimics, peroxidase mimics, etc.) are discussed. The catalytic mechanisms are also discussed if they have been elucidated. Representative examples for applications, from biosensing to therapeutics, are covered.

Keywords Nanozymes • Artificial enzymes • Enzyme mimics • Carbon-based nanomaterials • Fullerene and derivatives • Graphene and derivatives • Carbon nanotubes • Peroxidase mimics • Superoxide dismutase mimics • Nuclease mimics

Carbon-based nanomaterials, such as fullerene, carbon nanotubes (CNTs), graphene, and their derivatives, have found broad applications in many areas. Owing to their interesting catalytic activities, they have been extensively studied to mimic various natural enzymes. In this chapter, we will discuss the nanozymes based on these carbon nanomaterials.

2.1 Fullerene and Derivatives

Fullerene and its derivatives were among the first nanomaterials that have been explored for mimicking natural enzymes [1, 2]. In the early 1990s, the light-induced oxidative DNA cleavage with a C₆₀ derivative (i.e., C₆₀-1) was studied, indicating that fullerene could mimic natural nuclease [1]. A few years later, the superoxide dismutase (SOD) mimicking activity of derivatized C₆₀ was investigated, which led to the long-lasting research interests in fullerene-based nanozymes till today. Fullerene and its derivatives have also been used to mimic other enzymes besides nuclease and SOD.

2.1.1 Fullerene and Derivatives as Nuclease Mimics

Nuclease catalyzes the cleavage of phosphodiester bond between two nucleotides in a nucleic acid. Pristine fullerenes including C_{60} are not water soluble, which makes them impossible to mimic enzymes in aqueous solution. Therefore, fullerenes have been solubilized by introducing hydrophilic moieties. Nakamura group have made water-soluble C_{60} -1 and studied its photoinduced biochemical activities (Fig. 2.1) [1]. Interestingly, they established that the fullerene carboxylic acid (i.e., C_{60} -1) oxidatively cleaved DNA under light irradiation. Since C_{60} -1 did not bind to the DNA to be cleaved, the cleavage was random. To address this issue, Hélène, Nakamura and coworkers synthesized C_{60} -2, which had a 14-mer DNA sequence

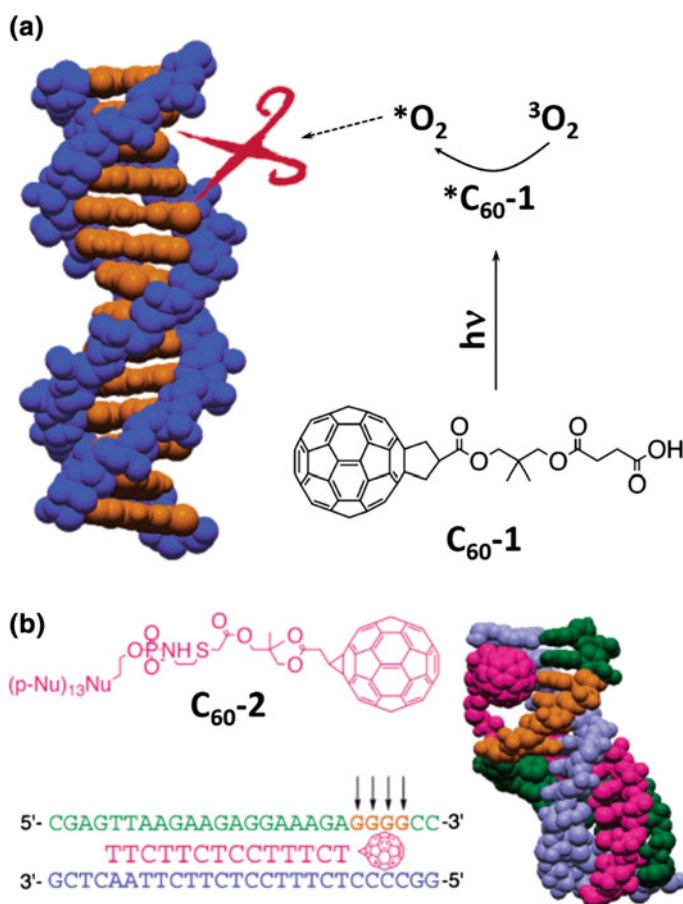


Fig. 2.1 Fullerene derivatives as nuclease mimics. **a** Light-induced cleavage of DNA with the fullerene derivative C_{60} -1. **b** Selective cleavage of DNA by forming a triplex with the fullerene DNA conjugate C_{60} -2. Adapted from Ref. [2], Copyright 2003, with permission from American Chemical Society

complementary to the target DNA (Fig. 2.1) [3]. By forming a triplex, the selective cleavage at guanine-rich sites was achieved. There are other ways to make the selective cleavage possible. For instance, by conjugating fullerenes with DNA intercalators (such as acridine), the formed fullerene derivative could enhance DNA cleavage activity compared with the parent fullerene [4]. These early studies have established that water-soluble fullerene derivatives could mimic nuclease.

2.1.2 Fullerene and Derivatives as SOD Mimics

(a) Fullerenes as SOD mimics: in vitro activities and mechanisms

Reactive oxygen species (ROS) plays both beneficial and harmful roles in living systems. Superoxide anion, one of ROS, could cause tissue injury and associated inflammation if it were not properly regulated. In nature, SOD has been evolved to catalyze the dismutation of superoxide anions into hydrogen peroxide and molecular oxygen and thus protect living systems from the superoxide anion-induced damage. To overcome the limits of natural SOD (such as limited stability and high cost), great efforts have been devoted to developing SOD mimics. The SOD-mimicking activities of fullerenes have been established by the seminal work from Choi and coworkers and have since been extensively studied [5].

Inspired by the early discovery that C_{60} could act as a radical sponge, Choi et al. studied the neuroprotective activities of two polyhydroxylated C_{60} (i.e., $C_{60}(OH)_{12}$ and $C_{60}(OH)_nO_m$, $n = 18-20$, $m = 3-7$ hemiketal groups) [5, 7]. Surprisingly, both of the two fullerene derivatives could scavenge free radicals and thus reduce excitotoxic and apoptotic death of cultured cortical neurons. Later, they identified that $C_{60}[C(COOH)_2]_3$ with C_3 symmetry ($C_{60}-C_3$) was more effective toward neuron protection [8]. Since superoxide anion could be eliminated via either a stoichiometric scavenging mechanism or a SOD-like catalytic mechanism, systematic studies including electron paramagnetic resonance (EPR) were carried out to confirm the SOD-mimicking activity of $C_{60}-C_3$ [6]. The possible stoichiometric scavenging mechanism was ruled out due to the following facts: first, no structural modifications to $C_{60}-C_3$ were observed; second, the production of oxygen and hydrogen peroxide was detected; and the absence of EPR active (paramagnetic) products. By combining the experimental results with computational data, a catalytic mechanism for SOD-like activity of $C_{60}-C_3$ was proposed (Fig. 2.2). The proposed mechanism was supported by other studies using dendritic C_{60} derivatives and other computational studies [9, 10].

The neuroprotective effects of fullerene-based SOD mimics were also studied using several other cell lines. For instance, methionine-modified C_{60} could protect SH-SY5Y neuroblastoma cells from lead ions (Pb^{2+}) induced oxidative damage and thus improved the cell survival [11].

Though water soluble fullerenes are usually required for enzyme-mimicking studies, it has been demonstrated that pristine C_{60} aqueous suspension was not only

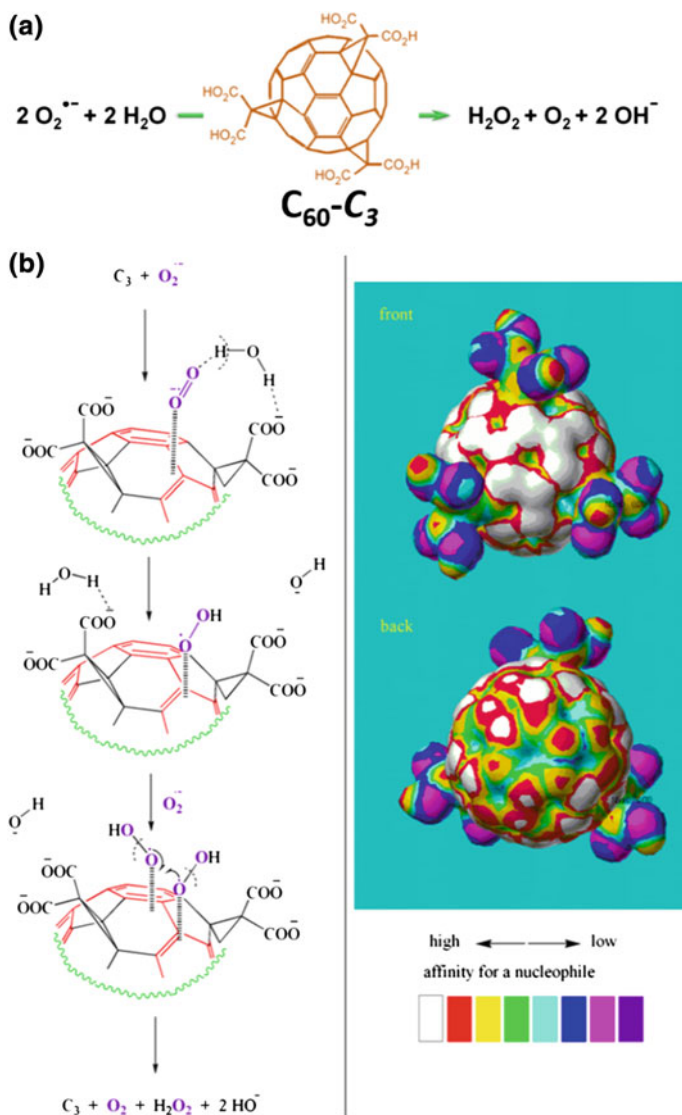


Fig. 2.2 Derivatized C_{60} as SOD mimics. **a** $\text{C}_{60}\text{-C}_3$ as a SOD mimic for catalytically converting superoxide anion into hydrogen peroxide, water, and hydroxyl. **b** The proposed catalytic mechanism. Adapted from Ref. [6], Copyright 2004, with permission from Elsevier

biocompatible but also showed protective effects on liver injury [12]. Besides derivatization, fullerenes could also be solubilized by using the similar strategies for hydrophobic drug solubilization. For instance, pristine C_{60} has been solubilized in olive oil for various applications [13].

(b) *Fullerenes as SOD mimics: in vivo applications*

To conclusively demonstrate that $C_{60}-C_3$ could work in living system as a SOD mimic, Dugan et al. employed SOD2 knockout mice as an *in vivo* model to investigate the therapeutic efficacy of $C_{60}-C_3$ (Fig. 2.3) [6]. The SOD2 knockout mice would die in utero or within a few days after birth owing to mitochondria damage by oxidative species. Therefore, they were suitable models to evaluate the *in vivo* effects of SOD mimics. It showed that the life span of the SOD2 defective mice could be extended by 300 % when $C_{60}-C_3$ was administrated both in utero and postnatally, demonstrating the $C_{60}-C_3$ could be functional alternatives to SOD2 in the studied mice. SOD2 is a manganese SOD localized in the mitochondria. Further immunostaining indeed revealed that $C_{60}-C_3$ was uptaken and localized to mitochondria [6].

These results indicated that fullerenes with SOD-mimicking activities (such as $C_{60}-C_3$) may hold translational promise for treating several diseases in future.

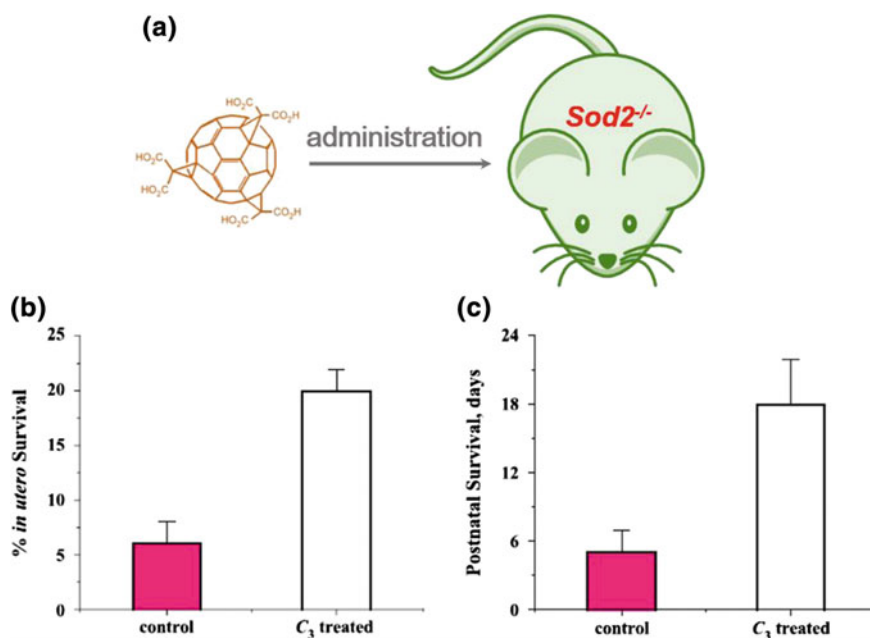


Fig. 2.3 **a** Treatment of SOD2 knockout mice with $C_{60}-C_3$. **b** Percentage of *Sod2*^{-/-} pups born to *Sod2*^{+/-} parents. Pregnant dams were given $C_{60}-C_3$ in their drinking water starting at Day 14–15 of pregnancy. Control dams received dilute red food coloring. The percentages of *Sod2*^{-/-} pups, per litter, born to control versus $C_{60}-C_3$ -treated dams were, respectively, 6 ± 2 % (controls, 11 L) and 20 ± 2 % (C₃, 9 L) (mean ± standard error of mean, with $p = 0.03$ by t test, and $p = 0.04$ by the nonparametric Wilcoxon rank sum test; the theoretical expected percentage is 25 %), indicating *in utero* rescue of some *Sod2*^{-/-} embryos. **c** Survival (days) of *Sod2*^{-/-} pups treated with daily subcutaneous injection of $C_{60}-C_3$ or color-matched food coloring until death. Values are means ± standard error of mean, * $p < 0.05$ by t test, $n = 9$, $C_{60}-C_3$ versus $n = 7$, vehicle. Adapted from Ref. [6], Copyright 2004, with permission from Elsevier

2.1.3 Fullerene Derivatives as Peroxidase Mimics

A few studies also showed that fullerenes could mimic peroxidase [14, 15]. For instance, the peroxidase-mimicking activity of $C_{60}[C(COOH)_2]_2$ was demonstrated by its catalyzed oxidation of 3,3',5,5'-tetramethylbenzidine (TMB) with H_2O_2 [15].

2.2 Graphene and Derivatives

Peroxidase catalyzes the oxidation of its substrates with H_2O_2 into oxidized products. The products are usually either colored or fluorescent, which enables peroxidase for a wide range of bioanalytical and biomedical applications. The peroxidase-mimicking activities of nanomaterials were initially studied with Fe_3O_4 nanoparticles by Yan and coworkers in 2007 [16]. Inspired by Yan's work, Wang et al. developed a general sensing strategy using Fe_3O_4 nanoparticles-based peroxidase mimic in 2008 (*see detailed discussion in Chap. 4*) [17]. Since then, lots of different nanomaterials have been investigated to mimic peroxidase. Among them, graphene and its various derivatives have showed great promise in mimicking peroxidase.

Graphene and its derivatives with peroxidase-mimicking activities can be roughly classified into two types. For the first type, the activities are solely from graphene or its derivatives. For the second type, the activities are either from the catalysts assembled onto graphene (or its derivatives) or from the synergistic effects of both the decorated catalysts and graphene (or its derivatives). Note: other enzyme-mimicking activities of graphene and its derivatives still remain to be investigated [18].

2.2.1 Graphene and Its Derivatives as Peroxidase Mimics

The peroxidase-mimicking activities have been studied mainly with graphene derivatives since pure graphene without any modifications is not water soluble. Qu and coworkers reported the intrinsic peroxidase-mimicking activity of graphene oxide with carboxyl modifications (GO-COOH) [19]. The activity was first demonstrated by the catalytic oxidation of TMB with H_2O_2 in the presence of GO-COOH (Fig. 2.4). The kinetic studies revealed that GO-COOH had higher affinity toward TMB in comparison with natural peroxidase. Interestingly, the GO-COOH catalyzed reactions proceeded via a ping-pong mechanism, which was the same as that for natural peroxidase. Since they did not detect trace amount of metal catalysts, they attributed the observed catalytic activity to the GO-COOH itself. No mechanism responsible for the catalytic activity was proposed, though it suggested that electron transfer from GC-COOH to H_2O_2 may be involved. By

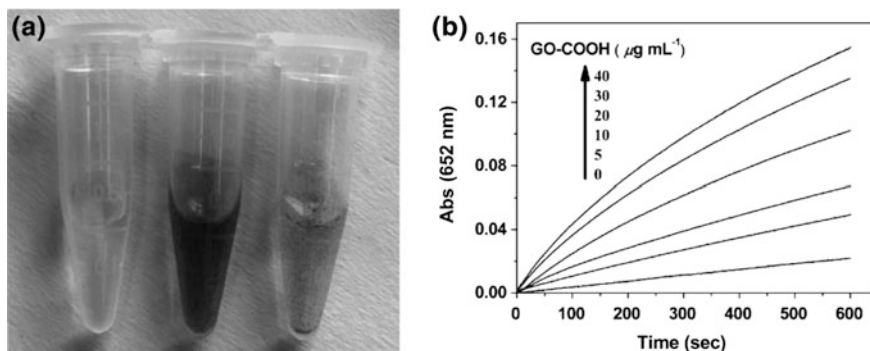
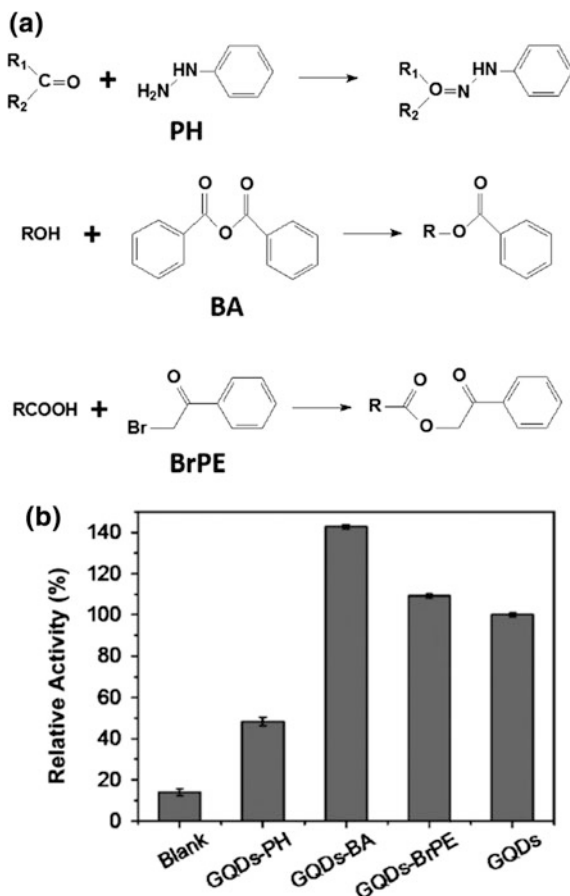


Fig. 2.4 Carboxyl-modified graphene oxide as peroxidase mimic. **a** Typical photographs of the reaction solutions incubated at room temperature in pH 5.0 phosphate buffer (from left to right): (1) 50 mM H_2O_2 and 800 μM TMB, colorless; (2) 40 mg/mL GO-COOH, black; (3) 50 mM H_2O_2 , 800 mM TMB and 40 mg mL/mL GO-COOH, turning blue. **b** The time-dependent absorbance changes at 652 nm in the absence (black) or presence of different concentrations of GO-COOH in pH 5.0 phosphate buffer at room temperature. Reprinted from Ref. [19], Copyright 2010, with permission from John Wiley and Sons

combining with natural glucose oxidase (GO_x), the glucose in diluted blood and fruit juice samples was successfully detected using the GC-COOH-based peroxidase mimic [19].

Graphene derivatives and many other carbon-based nanomaterials have rich oxygenated functional moieties (such as hydroxyl, ketone, carboxyl, epoxide, etc.). These functional moieties may play key roles in their enzyme-mimicking activities. To figure out the possible functional moieties responsible for the peroxidase-mimicking activity of a graphene derivative called graphene quantum dots (GQDs), several reagents were employed to selectively deactivate these functional moieties (Fig. 2.5) [20]. GQDs are small pieces of graphene derivative with fluorescent properties. It has ketone, hydroxyl, and carboxyl groups on the surface. These three groups can selectively react with phenylhydrazine (PH), benzoic anhydride (BA), and 2-bromo-1-phenylethanone (BrPE) respectively (Fig. 2.5). After treatment with PH, BA, BrPE, the peroxidase-mimicking activities of the treated GQDs were studied. As shown in Fig. 2.5b, the activity of PH-treated GQDs was significantly inhibited while the activity of BA-treated GQDs was enhanced. The activity of BrPE-treated GQDs remained almost the same as the untreated GQDs. Using a HO^\bullet specific fluorescent probe, the formation of HO^\bullet was confirmed during the catalytic reaction. Further kinetic measurements and theoretical calculation were also carried out. Taking together, these results suggested that ketone groups were the catalytically active sites and the carboxyl groups were the substrate binding sites. The hydroxyl groups, on the other hand, played an inhibitory role. It may be applicable to other carbon nanomaterials-based peroxidase mimics, which also have such oxygenated moieties.

Fig. 2.5 Deciphering peroxidase-mimicking activity of GQDs. **a** Reactions involved in selectively deactivating functional moieties on GQDs. **b** Relative catalytic activities of GQDs treated with different reagents. Adapted from Ref. [20], Copyright 2015, with permission from John Wiley and Sons



Since HO^\bullet was involved in peroxidase-mimicking activity of GQDs, they have showed antibacterial activity even in the low level of H_2O_2 . Both Gram-positive (*Staphylococcus aureus*) and Gram-negative (*Escherichia coli*) bacteria could be inhibited with the GQDs. The in vivo antibacterial efficacy was then evaluated using a mouse injury model, showing that the combination of GQDs with H_2O_2 exhibited the best therapeutic effects compared with saline, H_2O_2 , and GQDs [21].

The water solubility and stability of GO could be further enhanced by coating with polymers. To this end, chitosan, a cationic polysaccharide, was used to coat GO. The obtained chitosan-GO showed improved stability toward catalytic oxidation of TMB with H_2O_2 . Interestingly, it was found that the peroxidase-mimicking activity of the chitosan-GO was regulated by light [22]. Under visible light irradiation, the catalytic activity was turned on. More, the coated chitosan could interact with concanavalin A (Con A) via a multivalent manner, and the interaction would induce the aggregation of chitosan-GO. Such aggregation in turn reduced the activity of the nanozyme. Glucose, however, could compete for the

binding sites of chitosan on Con A due to the stronger interaction between glucose and Con A. Therefore, the presence of glucose would disassemble the chitosan–GO/Con A aggregates and thus recover the catalytic activity. Based on this phenomenon, a facile phototriggered method for glucose detection was developed. A linear range of 2.5–5.0 mM for glucose was achieved [22].

2.2.2 Decorated Graphene (or Its Derivatives) as Peroxidase Mimics

The large surface area of graphene and its derivatives provides a good opportunity to decorate them with various functional molecules and nanomaterials. As mentioned above, for such decorated graphene (or its derivatives), the peroxidase-mimicking activities could be originated from either the assembled catalyst itself or the catalyst/graphene (or its derivatives) assemblies.

In their seminal report, Dong and coworkers assembled hemin onto reduced GO (denoted as rGO) to form hemin–rGO complex and studied its peroxidase-mimicking activity (Fig. 2.6). The rGO was obtained by reducing GO with hydrazine. Then the hemin–rGO was prepared through the π - π stacking interaction between hemin and rGO. Compared with hemin–rGO, rGO showed almost negligible activity. Therefore, the peroxidase-mimicking activity of the hemin–rGO was mainly attributed to the assembled hemin. As shown in Fig. 2.6, the hemin–rGO-based nanozyme could catalyze the oxidation of TMB, ABTS (2,2'-azinobis (3-ethylbenzothiozoline)-6-sulfonic acid, and OPD (o-phenylenediamine) into the corresponding colored products with H_2O_2 . Kinetic studies revealed that the hemin–rGO catalyzed reaction also followed a ping-pong mechanism [23].

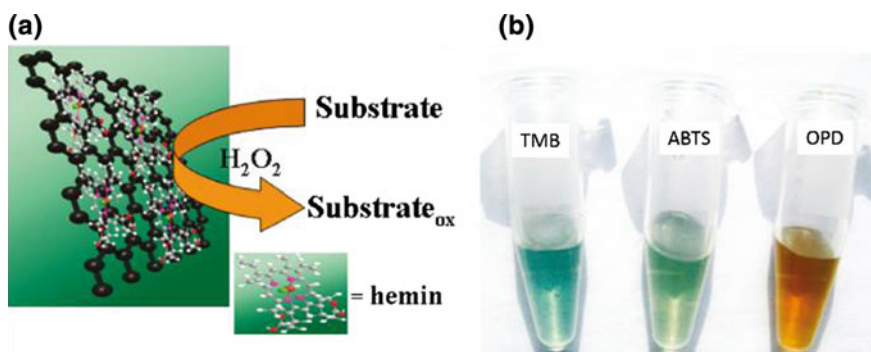


Fig. 2.6 Hemin-decorated rGO as peroxidase mimic. **a** Schematic illustration of peroxidase-like activity of hemin–rGO. **b** Hemin–rGO catalyzed oxidation of various peroxidase substrates with H_2O_2 to the corresponding colored products. Adapted from Ref. [23], Copyright 2011, with permission from American Chemical Society

It is known that single-stranded DNA (ssDNA) and double-stranded DNA (dsDNA) have different affinity toward various nanomaterials [24]. ssDNA binds tightly onto graphene (or its derivatives) while dsDNA binds weakly. Such a difference could be further amplified by salt-induced aggregation. In the presence of high concentration of salt (such as NaCl), ssDNA protects graphene (or its derivatives) from aggregation while dsDNA cannot. Based on this phenomenon, Dong et al. went on further to develop a label-free colorimetric method for single-nucleotide polymorphisms (SNPs) (Fig. 2.7) [23]. The probe ssDNA could stabilize the hemin-rGO and thus retained its peroxidase-mimicking activity. When the complementary target ssDNA was hybridized with the probe ssDNA, the formed dsDNA could not stabilize the hemin-rGO, which led to significant inhibition of its peroxidase-mimicking activity and produced the weakest signal. When a target ssDNA with a single-base mismatch was introduced, the formed duplex could partially protect the hemin-rGO from aggregation and thus retained part of its peroxidase-mimicking activity. This in turn resulted in the signal with medium intensity. As shown in Fig. 2.7, one could easily distinguish the single-base mismatched target DNA from the complementary one even with naked eyes [23].

This sensing strategy could be applicable to functional nucleic acids (such as aptamers) [24, 25]. An aptamer is an ssDNA or ssRNA that can specifically bind to its target. The binding usually induces a conformational change of the aptamer. Such a conformational change could in principle be sensed with hemin-rGO. For

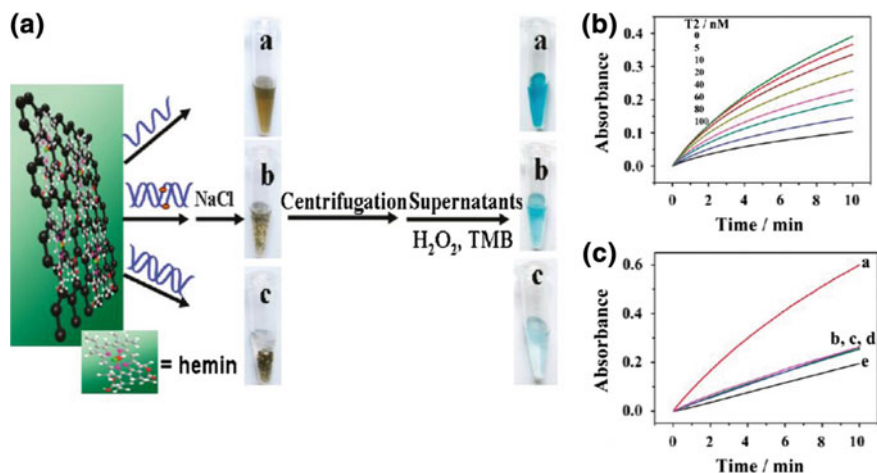


Fig. 2.7 Hemin-decorated rGO as peroxidase mimic for single-nucleotide polymorphisms. **a** Protocol for SNPs detection. (a) Probe ssDNA (no precipitation, dark blue), (b) single-base mismatched duplex DNA (small amount of precipitation, blue), and (c) complementary duplex DNA (much precipitation, light blue). **b** Time-dependent absorbance changes in the presence of different amounts of target ssDNA. **c** Time-dependent absorbance changes with corresponding supernatant in (a) ssDNA, (b, c, d) single-base mismatched duplex DNA, and (e) complementary duplex DNA. Reprinted from Ref. [23], Copyright 2011, with permission from American Chemical Society

instance, when an aptamer for acetamiprid (an insecticide) was used to stabilize hemin-rGO, the nanozyme showed high activity. However, the presence of acetamiprid would form the acetamiprid-aptamer complex, which did not protect the hemin-rGO efficiently. Therefore, the nanozyme's activity was significantly inhibited due to the aggregation. With this sensing strategy, as low as 40 nM acetamiprid was detected [26]. Other targets of interests can also be detected when the corresponding aptamers are used.

The synergistic effects were observed for numerous decorated graphene (or its derivatives) [27–35]. Among GO, rGO, AuNPs, the mixture of rGO and AuNPs, and the gold nanoparticles-decorated rGO (denoted as AuNPs@rGO), AuNPs@rGO exhibited the highest peroxidase-mimicking activity. As shown in Fig. 2.8, the significantly enhanced catalytic activity of the AuNPs@rGO was attributed to the synergistic effects. Careful study suggested that the synergistic effects were due to: (a) the strong interaction between Au 5d of AuNPs and C 2p of

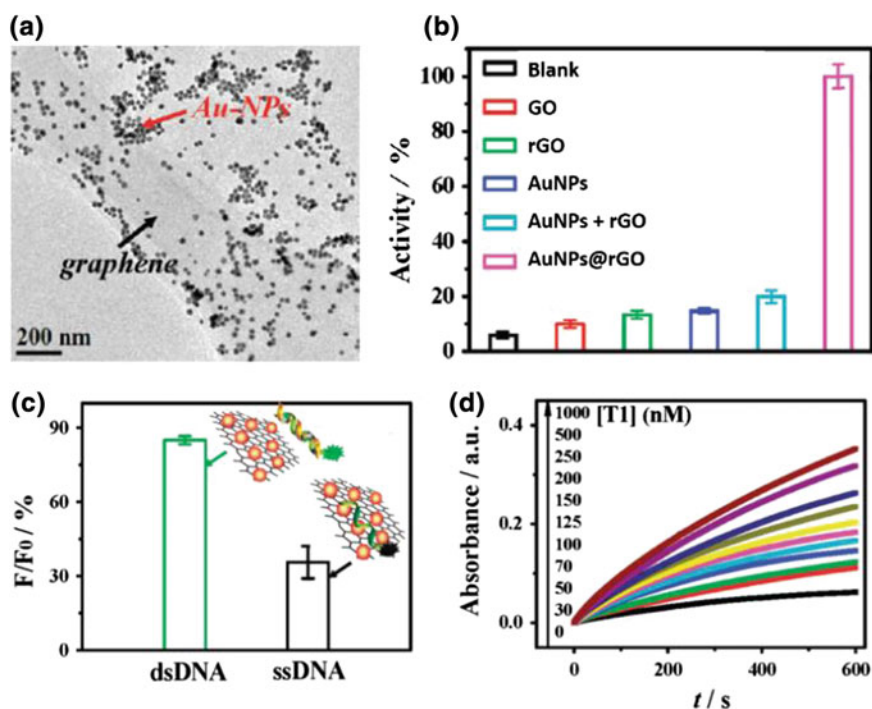


Fig. 2.8 AuNPs@rGO with synergistic peroxidase-mimicking activity and its use for DNA sensing. **a** TEM (transmission electron microscopy) image of AuNPs@rGO. **b** Peroxidase-mimicking activities of various nanomaterials. **c** Comparison of fluorescent retention ratio of FAM-labeled probe ssDNA and the corresponding dsDNA after incubated with AuNPs@rGO. **d** Time-dependent absorbance changes with varying concentrations of target ssDNA. Adapted from Ref. [27], Copyright 2012, with permission from American Chemical Society

rGO at the interface, which was favorable to H_2O_2 and HO^\cdot absorption; and (b) the modified electronic structure and Fermi level of rGO owing to the above-mentioned interfacing, which in turn resulted in the n-type doping of rGO and accelerated the catalytic reactions [27]. More, by further exploring the different affinities of ssDNA and dsDNA toward the AuNPs@rGO, a general analytical strategy for target DNA was developed (Fig. 2.8). The ssDNA specific nuclease (such as S1 nuclease) was also successfully detected using the developed method, where the presence of S1 nuclease would cleave the probe ssDNA into small fragments and thus recover the nanozyme's activity. If an aptamer was used as the probe ssDNA, the corresponding target (such as insulin) could be detected [27].

A hybrid called GSF@AuNPs with peroxidase-mimicking activity was prepared by in situ formation of AuNPs onto sandwich-like mesoporous silica/rGO. The silica/rGO was pre-conjugated with folic acid for tumor cell recognition [29]. The nanozyme was then used for detection of cancer cells with overexpressed folate receptor. For instance, rapid detection of HeLa cells was achieved. More, since HO^\cdot was generated during the catalysis, the nanozyme was also used to selectively kill cancer cells with the help of either exogenous or endogenous H_2O_2 [29].

Chen and coworkers prepared PtNPs decorated GO (i.e., PtNPs/GO) and further modified it with folic acid [36]. Based on the peroxidase-mimicking activity of the folic acid-PtNPs/GO, a colorimetric assay for cancer cells was developed (Fig. 2.9). With the developed assay, as few as 125 cancer cells have been detected by naked eyes.

By conjugating the monoclonal antibody for aflatoxin B_1 with a peroxidase-mimicking nanozyme, an electrochemical immunoassay for aflatoxin B_1 was reported by Tang et al. [32]. The nanozyme had a structure of PtNPs/CoTPP/rGO, in which CoTPP was 5,10,15,20-tetraphenyl-21H,23H-porphine cobalt. Aflatoxin B_1 is a highly toxic metabolite secreted by food fungi and its detection still needs rapid methods with high sensitivity and low cost. With

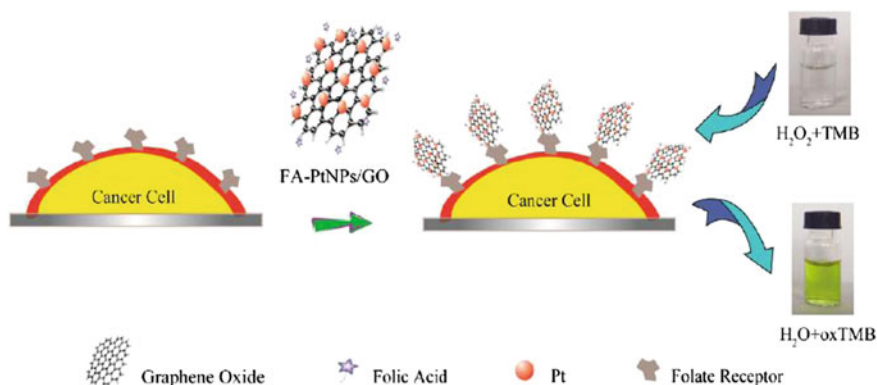


Fig. 2.9 Colorimetric detection of cancer cells with folic acid-PtNPs/GO as a peroxidase mimic. Reprinted from Ref. [36], Copyright 2014, with permission from American Chemical Society

the developed immunoassay, as low as 5.0 pg/mL of aflatoxin B₁ was successfully detected. Besides, the immunoassay has been used for analyzing real samples, such as the naturally contaminated peanut samples, showing good agreement with ELISA (enzyme-linked immunosorbent assay) kit [32].

Yu and coworkers reported a disposable electrochemical immunosensor based on peroxidase-mimicking nanozyme for cancer antigen 153 (CA153) detection [34]. Their nanozyme had a structure of ZnFe₂O₄@silica/GO (Fig. 2.10). The antibodies were conjugated onto the silica shell. Using a sandwich assay format, sensitive and selective detection of CA153 was achieved with a dynamic range from 10⁻³ to 200 U/mL and a detection limit of 2.8 × 10⁻⁴ U/mL. The fabricated immunosensor was further used to detect CA153 in serum samples and the results were consistent with the clinical ones.

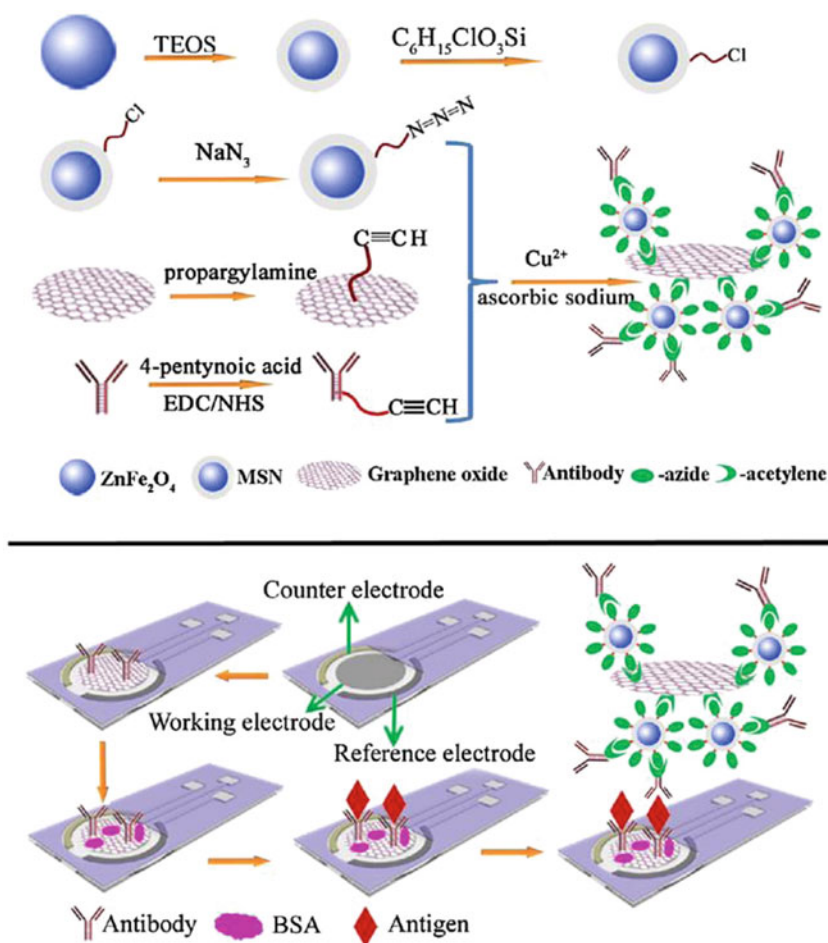


Fig. 2.10 Peroxidase-mimicking nanozyme and its use for disposable electrochemical immunosensor. Reprinted from Ref. [34], Copyright 2014, with permission from Elsevier

2.3 Carbon Nanotubes

CNTs as well as decorated CNTs have been used to mainly mimic peroxidase though other CNT-based enzyme mimics were also reported [37, 38].

2.3.1 Carbon Nanotubes as Peroxidase Mimics

Qu and coworkers reported the peroxidase-mimicking activity of single-walled carbon nanotubes (SWNTs) [39]. The activity of SWNTs was investigated by catalytic oxidation of TMB with H_2O_2 . Since metal catalysts are usually used to grow SWNTs, a trace amount of metal catalyst residues rather than SWNTs themselves may be responsible for the mimicking activity. To address this concern, the sonication-assisted washing with mixed acids (i.e., a mixture of concentrated sulfuric and nitric acids) was carried out to completely remove the metal residues (i.e., Co). It was found that pristine SWNTs and treated SWNTs did not show any significant differences in their catalytic activities. This confirmed that the peroxidase-mimicking activity of SWNTs was from the SWNTs themselves instead of the metal residues. By exploring the different affinities of ssDNA and dsDNA toward SWNTs, they developed a colorimetric assay for DNA detection [39].

It should be noted that in the above study, only the effect of Co on SWNTs' peroxidase-mimicking activity was tested. Other metal residues may have different effects. Zhu and coworkers indeed found that Fe content in the helical CNTs played an important role in their catalytic activities [40]. As shown in Fig. 2.11, the more Fe content of helical CNT was, the higher its peroxidase-mimicking activity of helical CNT was. Even for the helical CNT with the lowest amount of Fe, its activity was still higher than that of MWNTs (multiwalled CNTs). Zhu's and Qu's results suggest that more systematic studies are needed to decipher the exact mechanisms of CNTs' enzyme-mimicking activities. Zhu et al. then fabricated an electrochemical sensor using the helical CNTs as peroxidase mimic for H_2O_2 detection [40].

Like graphene, the decoration of CNTs could also synergistically enhance their peroxidase-mimicking activities. When MWNTs were decorated with magnetic silica nanoparticles, the decorated MWNTs exhibited higher peroxidase-mimicking activity compared with the individual components (i.e., MWNTs and magnetic silica nanoparticles, respectively) [41]. Since the decoration of magnetic silica nanoparticles onto MWNTs was achieved by the Cu^{2+} -mediated click chemistry, a colorimetric assay for Cu^{2+} was proposed (Fig. 2.12). The decorated MWNTs could be concentrated by a magnet and then used to oxidize TMB to its colored products. On the other hand, the undecorated MWNTs would be washed away and only the magnetic silica nanoparticles would be concentrated by a magnet. The latter exhibited much lower catalytic activity compared with the decorated

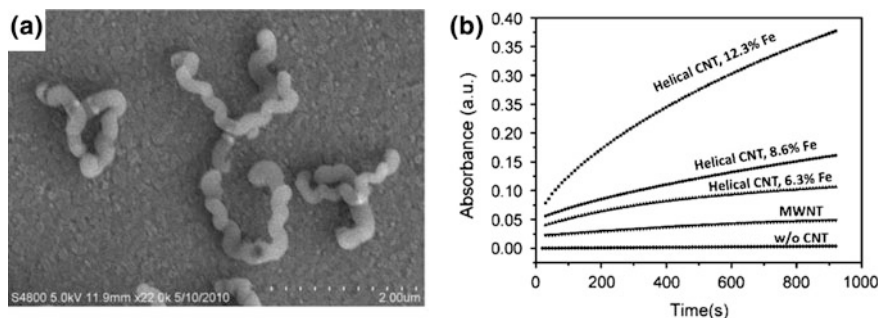


Fig. 2.11 Peroxidase-mimicking activity of helical CNTs. **a** SEM (scanning electron microscopy) image of helical CNTs. **b** Peroxidase-mimicking activities of helical CNTs with different Fe contents as well as MWNTs. The catalytic reaction without CNTs was shown as a control. Adapted from Ref. [40], Copyright 2011, with permission from John Wiley and Sons

MWNTs. Via such a sensing strategy, high sensitive and selective detection of Cu^{2+} has been carried out [41].

Other decorated CNTs with synergistically enhanced peroxidase-mimicking activities have also been developed and used to detect biologically important targets

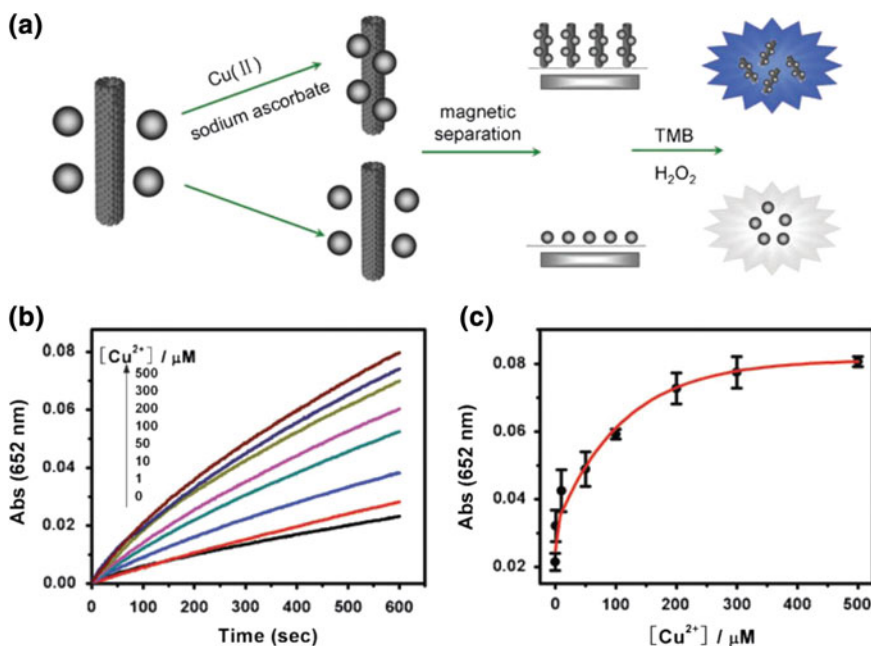


Fig. 2.12 Cu^{2+} detection using magnetic silica nanoparticles clicked on MWNTs. **a** The sensing mechanism. **b** The time-dependent absorbance changes in the absence (black) or presence of different concentration of Cu^{2+} . **c** Calibration curve for variable concentrations of Cu^{2+} . The error bars represent the standard deviation of three measurements. Reprinted from Ref. [41], Copyright 2010, with permission from Royal Society of Chemistry

(also see Tables A1 and A2). For example, when MWNTs were filled with Prussian blue nanoparticles, the formed nanozyme has been used for colorimetric detection of H_2O_2 [42]. When the nanozyme was further combined with glucose oxidase, it has been successfully used for glucose detection with a linear range of 1 μM to 1.0 mM and a detection limit of 200 nM. The potential practical application was demonstrated by detecting glucose in serum samples, showing satisfactory recoveries of 94–106 % [42]. Cholesterol levels in milk powder were evaluated by using ZnO nanoparticles-decorated CNTs as a peroxidase mimic [43]. Cholesterol was catalytically oxidized with cholesterol oxidase to produce H_2O_2 , which was then used for oxidizing ABTS into the colored product with the nanozyme. A colorimetric approach to detection of D-alanine was developed by using Au nanoparticles-decorated SWNTs as a peroxidase mimic [44]. D-alanine was catalytically oxidized with D-amino acids oxidase to produce H_2O_2 for the further oxidation of TMB. The proposed approach showed high selectivity and high sensitivity toward D-alanine detection.

A paper-based immunoassay was developed using ZnFe_2O_4 -decorated MWNTs as a peroxidase mimic [45]. Carcinoembryonic antigen (CEA) was chosen due to its correlation with cancer. The nanozymes-based immunoassay exhibited high sensitivity and robustness. More, the immunoassay has been used to detect CEA in clinical serum samples, showing consistent results compared with a commercialized ELISA method [45].

2.3.2 Carbon Nanotubes as Other Enzyme Mimics

As discussed above, it has been established that fullerenes can efficiently scavenge radicals due to their SOD-mimicking activities. Thus, it is reasonable to investigate the radical scavenging activities of CNTs. Tour and coworkers have studied the radical scavenging activities of several SWNTs (Fig. 2.13) [37]. They used butylated hydroxytoluene (BHT), a phenolic antioxidant, to modify the SWNTs. The anchored BHT would endow the SWNTs with radical scavenging activities. Pristine SWNT (SWNT-1) was not water soluble. Therefore, it was solubilized by either wrapping a polymer (such as Pluronic for SWNT-2) or introducing carboxyl moieties by mixed acid treatment/cleavage (i.e., SWNT-3). SWNT-3 was further modified with PEG (poly(ethylene glycol)) to produce SWNT-4, which was soluble in buffer.

The radical scavenging activities were evaluated by comparing with Trolox, a vitamin E derivate. The TME (Trolox mass equivalence) values were then determined. Unexpectedly, SWNT-4 without BHT modification exhibited nearly 40 times higher activity (Fig. 2.14). This indicated that SWNTs alone could act as antioxidants. For SWNT-5, amine-BHT was assembled via electrostatic interactions while amine-BHT was covalently conjugated for SWNT-6. Since electrostatic binding was more efficient than the covalent binding, more amine-BHT should bind onto SWNT-5 than SWNT-6. As expected, SWNT-5 showed higher radical scavenging activity than SWNT-6 did (Fig. 2.14). For SWNT-2 and SWNT-7, one

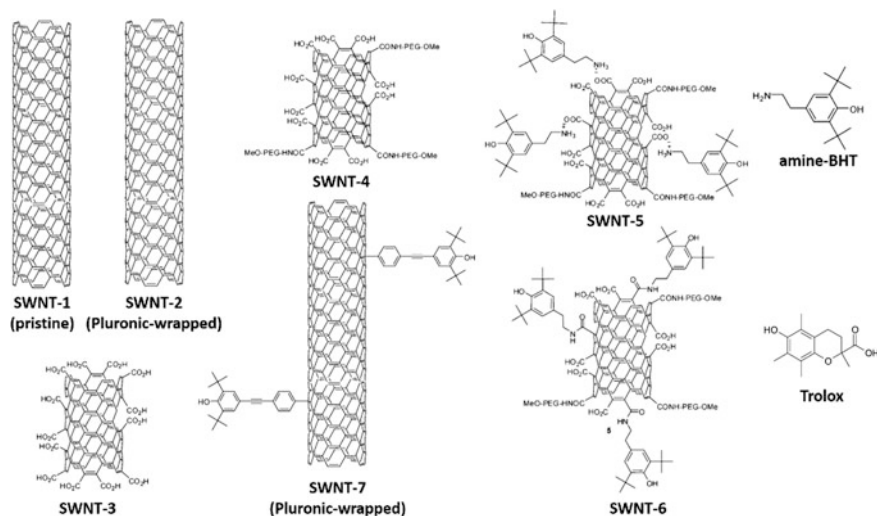


Fig. 2.13 SWNTs used for scavenging radicals. Adapted from Ref. [37], Copyright 2009, with permission from American Chemical Society

would expect that **SWNT-7** would have higher activity since it had extra BHT moieties. Surprisingly, **SWNT-7** exhibited lower activity when compared with **SWNT-2** (Fig. 2.14) [37]. This unexpected result indicated that pristine SWNTs had higher radical scavenging activities than BHT. This study demonstrated that SWNTs could act as potent antioxidant without acute cellular toxicity.

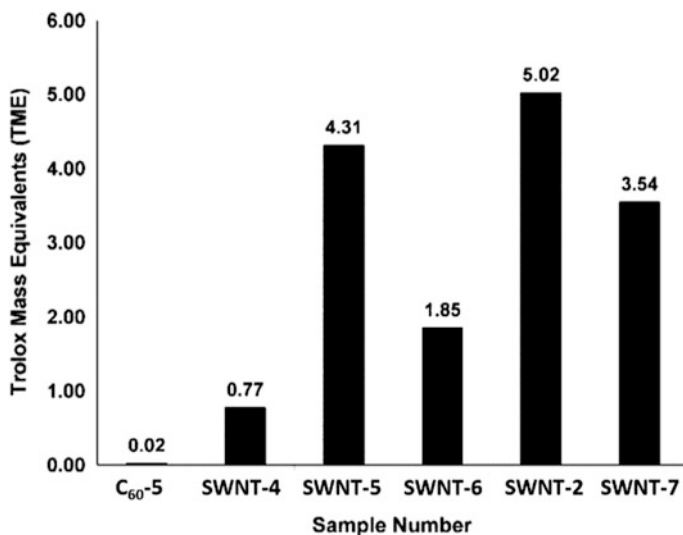


Fig. 2.14 Radical scavenging activities (i.e., the TME values) of the SWNTs studied. C₆₀-5 was also included for a comparison. Adapted from Ref. [37], Copyright 2009, with permission from American Chemical Society

Note that though it has established that fullerenes act as SOD mimic to scavenge radicals, whether CNTs share a similar SOD mimetic mechanism still remains to be investigated.

2.4 Other Carbon-Based Nanomaterials

Other carbon-based nanomaterials (such as carbon nanohorn, carbon nanodots, carbon nanoclusters, etc.) have also been used to mimic peroxidase and other enzymes [46–58].

2.4.1 Other Carbon Nanomaterials as Peroxidase Mimics

Several groups studied the peroxidase-mimicking activities of carbon nanohorns, carbon nanodots, etc. [46–48, 50–52, 58, 59]

For instance, Xu and coworkers demonstrated that carboxyl-functionalized single-walled carbon nanohorns exhibited peroxidase-like activity (Fig. 2.15) [46]. When the nanozyme was further combined with glucose oxidase, a facile colorimetric assay for glucose was developed. Carbon nanodots with an average size of 2.5 nm also showed peroxidase-mimicking activity and have been used for glucose sensing (Fig. 2.15c) [51]. The peroxidase-like activity of selenium-doped graphitic carbon nitride nanosheets was demonstrated and further explored for xanthine detection when facilitated with xanthine oxidase [52].

Using $[\text{Cu}_3(\text{BTC})_2]$ (BTC = 1,3,5-benzene tricarboxylate) as a precursor, copper nanoparticles-decorated carbon nanocomposite was fabricated via a one-pot thermolysis method (Fig. 2.15d) [47]. It demonstrated that the nanocomposite exhibited peroxidase mimetic activity. Ascorbic acid, a biologically important antioxidant, could competitively inhibit the catalytic oxidation of peroxidase substrate (such as TMB in this study). Based on this inhibition phenomenon, a colorimetric method for ascorbic acid was developed [47, 60]. The ascorbic acid content in tablets has been successfully determined with the nanozyme-based method [47].

2.4.2 Other Carbon Nanomaterials as SOD Mimics

The SOD-mimicking activities of nitrogen-doped carbon nanodots have been studied [58]. It demonstrated that primary amine were the optimal reagents for nitrogen doping. When the obtained nitrogen-doped carbon nanodots were added to H_2O_2 -treated cells, they would enhance the cell viability in a concentration-dependent manner. It suggested that the nitrogen-doped carbon nanodots protect cells from H_2O_2 -induced injury by eliminating the ROS and stimulating the native SOD expression [58].

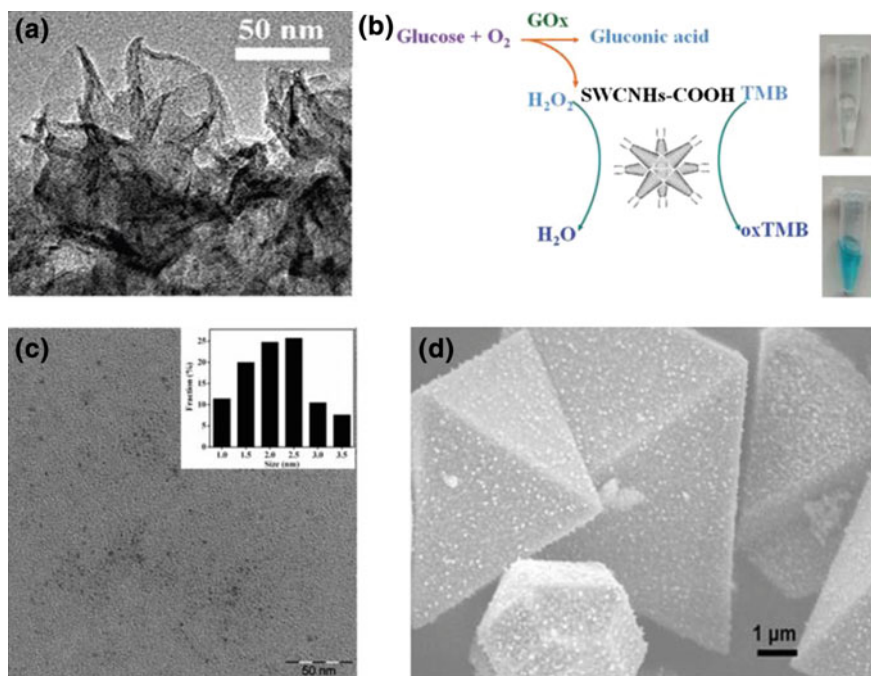


Fig. 2.15 Carbon nanomaterials as peroxidase mimics. **a** Single-walled carbon nanohorns as peroxidase mimic and **b** their use for glucose detection. **c** Carbon nanodots as peroxidase mimics. **d** Copper nanoparticles-decorated carbon as peroxidase mimics. **a** and **b** Reprinted from Ref. [46], Copyright 2015, with permission from Royal Society of Chemistry. **c** Reprinted from Ref. [51], Copyright 2011, with permission from Royal Society of Chemistry. **d** Reprinted from Ref. [47], Copyright 2014, with permission from John Wiley and Sons

References

1. Tokuyama, H., Yamago, S., Nakamura, E., Shiraki, T., & Sugiura, Y. (1993). Photoinduced biochemical-activity of fullerene carboxylic-acid. *Journal of the American Chemical Society*, 115, 7918–7919.
2. Nakamura, E., & Isobe, H. (2003). Functionalized fullerenes in water. The first 10 years of their chemistry, biology, and nanoscience. *Accounts of Chemical Research*, 36, 807–815.
3. Botorine, A. S., Tokuyama, H., Takasugi, M., Isobe, H., Nakamura, E., & Helene, C. (1994). Fullerene-oligonucleotide conjugates: Photoinduced sequence-specific DNA cleavage. *Angewandte Chemie-International Edition*, 33, 2462–2465.
4. Yamakoshi, Y. N., Yagami, T., Sueyoshi, S., & Miyata, N. (1996). Acridine adduct of 60 fullerene with enhanced DNA-cleaving activity. *Journal of Organic Chemistry*, 61, 7236–7237.
5. Dugan, L. L., Gabrielsen, J. K., Yu, S. P., Lin, T. S., & Choi, D. W. (1996). Buckminsterfullerenol free radical scavengers reduce excitotoxic and apoptotic death of cultured cortical neurons. *Neurobiology of Disease*, 3, 129–135.
6. Ali, S. S., Hardt, J. I., Quick, K. L., Kim-Han, J. S., Erlanger, B. F., Huang, T. T., et al. (2004). A biologically effective fullerene (C-60) derivative with superoxide dismutase mimetic properties. *Free Radical Biology and Medicine*, 37, 1191–1202.

7. Krusic, P. J., Wasserman, E., Keizer, P. N., Morton, J. R., & Preston, K. F. (1991). Radical reactions of C₆₀. *Science*, 254, 1183–1185.
8. Dugan, L. L., Turetsky, D. M., Du, C., Lobner, D., Wheeler, M., Almli, C. R., et al. (1997). Carboxyfullerenes as neuroprotective agents. *Proceedings of the National Academy of Sciences of the United States of America*, 94, 9434–9439.
9. Liu, G.-F., Filipovic, M., Ivanovic-Burmazovic, I., Beuerle, F., Witte, P., & Hirsch, A. (2008). High catalytic activity of dendritic C₆₀ monoadducts in metal-free superoxide dismutation. *Angewandte Chemie-International Edition*, 47, 3991–3994.
10. Osuna, S., Swart, M., & Sola, M. (2010). On the mechanism of action of fullerene derivatives in superoxide dismutation. *Chemistry-A European Journal*, 16, 3207–3214.
11. Chen, T., Li, Y.-Y., Zhang, J.-L., Xu, B., Lin, Y., Wang, C.-X., et al. (2011). Protective effect of C₆₀-methionine derivate on lead-exposed human SH-SY5Y neuroblastoma cells. *Journal of Applied Toxicology*, 31, 255–261.
12. Gharbi, N., Pressac, M., Hadchouel, M., Szwarc, H., Wilson, S. R., & Moussa, F. (2005). 60 Fullerene is a powerful antioxidant in vivo with no acute or subacute toxicity. *Nano Letters*, 5, 2578–2585.
13. Baati, T., Bourasset, F., Gharbi, N., Njim, L., Abderrabba, M., Kerkeni, A., et al. (2012). The prolongation of the lifespan of rats by repeated oral administration of 60 fullerene. *Biomaterials*, 33, 4936–4946.
14. Okuda, K., Mashino, T., & Hirobe, M. (1996). Superoxide radical quenching and cytochrome c peroxidase-like activity of C₆₀-dimalonic acid, C₆₂(COOH)₄. *Bioorganic & Medicinal Chemistry Letters*, 6, 539–542.
15. Li, R. M., Zhen, M. M., Guan, M. R., Chen, D. Q., Zhang, G. Q., Ge, J. C., et al. (2013). A novel glucose colorimetric sensor based on intrinsic peroxidase-like activity of C₆₀-carboxyfullerenes. *Biosensors & Bioelectronics*, 47, 502–507.
16. Gao, L. Z., Zhuang, J., Nie, L., Zhang, J. B., Zhang, Y., Gu, N., et al. (2007). Intrinsic peroxidase-like activity of ferromagnetic nanoparticles. *Nature Nanotechnology*, 2, 577–583.
17. Wei, H., & Wang, E. (2008). Fe₃O₄ magnetic nanoparticles as peroxidase mimetics and their applications in H₂O₂ and glucose detection. *Analytical Chemistry*, 80, 2250–2254.
18. Liu, T., Niu, X., Shi, L., Zhu, X., Zhao, H., & Lana, M. (2015). Electrocatalytic analysis of superoxide anion radical using nitrogen-doped graphene supported Prussian Blue as a biomimetic superoxide dismutase. *Electrochimica Acta*, 176, 1280–1287.
19. Song, Y., Qu, K., Zhao, C., Ren, J., & Qu, X. (2010). Graphene oxide: Intrinsic peroxidase catalytic activity and its application to glucose detection. *Advanced Materials*, 22, 2206–2210.
20. Sun, H. J., Zhao, A. D., Gao, N., Li, K., Ren, J. S., & Qu, X. G. (2015). Deciphering a nanocarbon-based artificial peroxidase: Chemical identification of the catalytically active and substrate-binding sites on graphene quantum dots. *Angewandte Chemie-International Edition*, 54, 7176–7180.
21. Sun, H., Gao, N., Dong, K., Ren, J., & Qu, X. (2014). Graphene quantum dots-band-aids used for wound disinfection. *ACS Nano*, 8, 6202–6210.
22. Wang, G. L., Xu, X. F., Wu, X. M., Cao, G. X., Dong, Y. M., & Li, Z. J. (2014). Visible-light-stimulated enzymelike activity of graphene oxide and its application for facile glucose sensing. *Journal of Physical Chemistry C*, 118, 28109–28117.
23. Guo, Y. J., Deng, L., Li, J., Guo, S. J., Wang, E. K., & Dong, S. J. (2011). Hemin-graphene hybrid nanosheets with intrinsic peroxidase-like activity for label-free colorimetric detection of single-nucleotide polymorphism. *ACS Nano*, 5, 1282–1290.
24. Wei, H., Li, B. L., Li, J., Wang, E. K., Dong, S. J. (2007) Simple and sensitive aptamer-based colorimetric sensing of protein using unmodified gold nanoparticle probes. *Chemical Communications*, 3735–3737.
25. Wei, H., Li, B. L., Li, J., Dong, S. J., & Wang, E. K. (2008). DNAzyme-based colorimetric sensing of lead (Pb²⁺) using unmodified gold nanoparticle probes. *Nanotechnology*, 19, 095501.

26. Yang, Z., Qian, J., Yang, X., Jiang, D., Du, X., Wang, K., et al. (2015). A facile label-free colorimetric aptasensor for acetamiprid based on the peroxidase-like activity of hemin-functionalized reduced graphene oxide. *Biosensors & Bioelectronics*, 65, 39–46.
27. Liu, M., Zhao, H. M., Chen, S., Yu, H. T., & Quan, X. (2012). Interface engineering catalytic graphene for smart colorimetric biosensing. *ACS Nano*, 6, 3142–3151.
28. Liu, M., Zhao, H. M., Chen, S., Yu, H. T., & Quan, X. (2012). Stimuli-responsive peroxidase mimicking at a smart graphene interface. *Chemical Communications*, 48, 7055–7057.
29. Maji, S. K., Mandal, A. K., Nguyen, K. T., Borah, P., & Zhao, Y. L. (2015). Cancer cell detection and therapeutics using peroxidase-active nanohybrid of gold nanoparticle-loaded mesoporous silica-coated graphene. *ACS Applied Materials & Interfaces*, 7, 9807–9816.
30. Wang, H., Li, S., Si, Y. M., Sun, Z. Z., Li, S. Y., & Lin, Y. H. (2014). Recyclable enzyme mimic of cubic Fe_3O_4 nanoparticles loaded on graphene oxide-dispersed carbon nanotubes with enhanced peroxidase-like catalysis and electrocatalysis. *Journal of Materials Chemistry B*, 2, 4442–4448.
31. Dutta, S., Ray, C., Mallick, S., Sarkar, S., Sahoo, R., Negishi, Y., et al. (2015). A gel-based approach to design hierarchical cus decorated reduced graphene oxide nanosheets for enhanced peroxidase-like activity leading to colorimetric detection of dopamine. *Journal of Physical Chemistry C*, 119, 23790–23800.
32. Shu, J., Qiu, Z., Wei, Q., Zhuang, J., & Tang, D. (2015). Cobalt-porphyrin-platinum-functionalized reduced graphene oxide hybrid nanostructures: A novel peroxidase mimetic system for improved electrochemical immunoassay. *Scientific Reports*, 5, 15113.
33. Ma, Z., Qiu, Y. F., Yang, H. H., Huang, Y. M., Liu, J. J., Lu, Y., et al. (2015). Effective synergistic effect of dipeptide-polyoxometalate-graphene oxide ternary hybrid materials on peroxidase-like mimics with enhanced performance. *ACS Applied Materials & Interfaces*, 7, 22036–22045.
34. Ge, S., Sun, M., Liu, W., Li, S., Wang, X., Chu, C., et al. (2014). Disposable electrochemical immunosensor based on peroxidase-like magnetic silica-graphene oxide composites for detection of cancer antigen 153. *Sensors and Actuators B-Chemical*, 192, 317–326.
35. Yan, X., Gu, Y., Li, C., Tang, L., Zheng, B., Li, Y., et al. (2016). Synergetic catalysis based on the proline tailed metalloporphyrin with graphene sheet as efficient mimetic enzyme for ultrasensitive electrochemical detection of dopamine. *Biosensors & Bioelectronics*, 77, 1032–1038.
36. Zhang, L. N., Deng, H. H., Lin, F. L., Xu, X. W., Weng, S. H., Liu, A. L., et al. (2014). In situ growth of porous platinum nanoparticles on graphene oxide for colorimetric detection of cancer cells. *Analytical Chemistry*, 86, 2711–2718.
37. Lucente-Schultz, R. M., Moore, V. C., Leonard, A. D., Price, B. K., Kosynkin, D. V., Lu, M., et al. (2009). Antioxidant single-walled carbon nanotubes. *Journal of the American Chemical Society*, 131, 3934–3941.
38. Zhang, B., He, Y., Liu, B., & Tang, D. (2014). NiCoBP-doped carbon nanotube hybrid: A novel oxidase mimetic system for highly efficient electrochemical immunoassay. *Analytica Chimica Acta*, 851, 49–56.
39. Song, Y., Wang, X., Zhao, C., Qu, K., Ren, J., & Qu, X. (2010). Label-free colorimetric detection of single nucleotide polymorphism by using single-walled carbon nanotube intrinsic peroxidase-like activity. *Chemistry-A European Journal*, 16, 3617–3621.
40. Cui, R., Han, Z., & Zhu, J.-J. (2011). Helical carbon nanotubes: Intrinsic peroxidase catalytic activity and its application for biocatalysis and biosensing. *Chemistry-A European Journal*, 17, 9377–9384.
41. Song, Y., Qu, K., Xu, C., Ren, J., & Qu, X. (2010). Visual and quantitative detection of copper ions using magnetic silica nanoparticles clicked on multiwalled carbon nanotubes. *Chemical Communications*, 46, 6572–6574.

42. Wang, T., Fu, Y. C., Chai, L. Y., Chao, L., Bu, L. J., Meng, Y., et al. (2014). Filling carbon nanotubes with prussian blue nanoparticles of high peroxidase-like catalytic activity for colorimetric chemo and biosensing. *Chemistry-A European Journal*, 20, 2623–2630.
43. Hayat, A., Haider, W., Raza, Y., & Marty, J. L. (2015). Colorimetric cholesterol sensor based on peroxidase like activity of zinc oxide nanoparticles incorporated carbon nanotubes. *Talanta*, 143, 157–161.
44. Haider, W., Hayat, A., Raza, Y., Chaudhry, A. A., Ihtesham Ur, R., & Marty, J. L. (2015). Gold nanoparticle decorated single walled carbon nanotube nanocomposite with synergistic peroxidase like activity for D-alanine detection. *RSC Advances*, 5, 24853–24858.
45. Liu, W. Y., Yang, H. M., Ding, Y. A., Ge, S. G., Yu, J. H., Yan, M., et al. (2014). Paper-based colorimetric immunosensor for visual detection of carcinoembryonic antigen based on the high peroxidase-like catalytic performance of ZnFe_2O_4 -multiwalled carbon nanotubes. *Analyst*, 139, 251–258.
46. Zhu, S. Y., Zhao, X. E., You, J. M., Xu, G. B., & Wang, H. (2015). Carboxylic-group-functionalized single-walled carbon nanohorns as peroxidase mimetics and their application to glucose detection. *Analyst*, 140, 6398–6403.
47. Tan, H. L., Ma, C. J., Gao, L., Li, Q., Song, Y. H., Xu, F. G., et al. (2014). Metal-organic framework-derived copper nanoparticle@carbon nanocomposites as peroxidase mimics for colorimetric sensing of ascorbic acid. *Chemistry-a European Journal*, 20, 16377–16383.
48. Liu, S., Tian, J. Q., Wang, L., Luo, Y. L., & Sun, X. P. (2012). A general strategy for the production of photoluminescent carbon nitride dots from organic amines and their application as novel peroxidase-like catalysts for colorimetric detection of H_2O_2 and glucose. *RSC Advances*, 2, 411–413.
49. Wang, X. H., Qu, K. G., Xu, B. L., Ren, J. S., & Qu, X. G. (2011). Multicolor luminescent carbon nanoparticles: Synthesis, supramolecular assembly with porphyrin, intrinsic peroxidase-like catalytic activity and applications. *Nano Research*, 4, 908–920.
50. Dong, Y. M., Zhang, J. J., Jiang, P. P., Wang, G. L., Wu, X. M., Zhao, H., et al. (2015). Superior peroxidase mimetic activity of carbon dots-Pt nanocomposites relies on synergistic effects. *New Journal of Chemistry*, 39, 4141–4146.
51. Shi, W. B., Wang, Q. L., Long, Y. J., Cheng, Z. L., Chen, S. H., Zheng, H. Z., et al. (2011). Carbon nanodots as peroxidase mimetics and their applications to glucose detection. *Chemical Communications*, 47, 6695–6697.
52. Qian, F. M., Wang, J. M., Ai, S. Y., & Li, L. F. (2015). As a new peroxidase mimetics: The synthesis of selenium doped graphitic carbon nitride nanosheets and applications on colorimetric detection of H_2O_2 and xanthine. *Sensors and Actuators B-Chemical*, 216, 418–427.
53. Samuel, E. L. G., Marciano, D. C., Berka, V., Bitner, B. R., Wu, G., Potter, A., et al. (2015). Highly efficient conversion of superoxide to oxygen using hydrophilic carbon clusters. *Proceedings of the National Academy of Sciences of the United States of America*, 112, 2343–2348.
54. Bitner, B. R., Marciano, D. C., Berlin, J. M., Fabian, R. H., Cherian, L., Culver, J. C., et al. (2012). Antioxidant carbon particles improve cerebrovascular dysfunction following traumatic brain injury. *ACS Nano*, 6, 8007–8014.
55. Marciano, D. C., Bitner, B. R., Berlin, J. M., Jarjour, J., Lee, J. M., Jacob, A., et al. (2013). Design of poly(ethylene glycol)-functionalized hydrophilic carbon clusters for targeted therapy of cerebrovascular dysfunction in mild traumatic brain injury. *Journal of Neurotrauma*, 30, 789–796.
56. Samuel, E. L. G., Duong, M. T., Bitner, B. R., Marciano, D. C., Tour, J. M., & Kent, T. A. (2014). Hydrophilic carbon clusters as therapeutic, high-capacity antioxidants. *Trends in Biotechnology*, 32, 501–505.
57. Nilewski, L. G., Sikkema, W. K. A., Kent, T. A., & Tour, J. M. (2015). Carbon nanoparticles and oxidative stress: Could an injection stop brain damage in minutes? *Nanomedicine*, 10, 1677–1679.

58. Xu, Z.-Q., Lan, J.-Y., Jin, J.-C., Dong, P., Jiang, F.-L., & Liu, Y. (2015). Highly photoluminescent nitrogen-doped carbon nanodots and their protective effects against oxidative stress on cells. *ACS Applied Materials & Interfaces*, 7, 28346–28352.
59. Clark, A., Zhu, A. P., Sun, K., & Petty, H. R. (2011). Cerium oxide and platinum nanoparticles protect cells from oxidant-mediated apoptosis. *Journal of Nanoparticle Research*, 13, 5547–5555.
60. Cheng, H., Wang, X., & Wei, H. (2015). Ratiometric electrochemical sensor for effective and reliable detection of ascorbic acid in living brains. *Analytical Chemistry*, 87, 8889–8895.

Nanozymes: Next Wave of Artificial Enzymes

Wang, X.; Guo, W.; Hu, Y.; Wu, J.; Wei, H.

2016, X, 127 p. 56 illus., 47 illus. in color., Softcover

ISBN: 978-3-662-53066-5